Biomaterials 140 (2017) 201–211

Contents lists available at ScienceDirect

Biomaterials

journal homepage: www.elsevier.com/locate/biomaterials

Linker-free covalent immobilization of heparin, SDF-1α, and CD47 on PTFE surface for antithrombogenicity, endothelialization and anti-inflammation

Ang Gao [a, b], Ruiqiang Hang [c], Wan Li [a], Wei Zhang [d], Penghui Li [b], Guomin Wang [a], Long Bai [c], Xue-Feng Yu [b], Huaiyu Wang [b, *], Liping Tong [b, **], Paul K. Chu [a, ***]

[a] Department of Physics and Materials Science, City University of Hong Kong, Tat Chee Avenue, Kowloon, Hong Kong, China
[b] Institute of Biomedicine and Biotechnology, Shenzhen Institutes of Advanced Technology, Chinese Academy of Sciences, Shenzhen, 518055, China
[c] Research Institute of Surface Engineering, Taiyuan University of Technology, Taiyuan, 030024, China
[d] Technical Institute of Physics and Chemistry, Chinese Academy of Sciences, Beijing, 100190, China

ARTICLE INFO

Article history:
Received 11 May 2017
Received in revised form
17 June 2017
Accepted 18 June 2017
Available online 20 June 2017

Keywords:
PTFE
Surface modification
Plasma immersion ion implantation
Covalent immobilization
Multi-functionalization

ABSTRACT

Small-diameter vascular grafts made of biomedical polytetrafluoroethylene (PTFE) suffer from the poor long-term patency rate originating from thrombosis and intimal hyperplasia, which can be ascribed to the insufficient endothelialization and chronic inflammation of the materials. Hence, bio-functionalization of PTFE grafts is highly desirable to circumvent these disadvantages. In this study, a versatile "implantation-incubation" approach in which the biomedical PTFE is initially modified by plasma immersion ion implantation (PIII) is described. After the N_2 PIII treatment, the surface of biomedical PTFE is roughened with nanostructures and more importantly, the abundant free radicals generated underneath the surface continuously migrate to the surface and react with environmental molecules. Taking advantage of this mechanism, various biomolecules with different functions can be steadily immobilized on the surface of PTFE by simple solution immersion. As examples, three typical biomolecules, heparin, SDF-1α, and CD47, are covalently grafted onto the PTFE. In addition to retaining the bioactivity, the surface-functionalized PTFE exhibits reduced thrombogenicity, facilitates the recruitment of endothelial progenitor cells, and even alleviates the inflammatory immune responses of monocytes-macrophages and is thus promising to the development of small-diameter prosthetic vascular grafts with good long-term patency.

1. Introduction

Prosthetic vascular grafts, particularly those made of expanded polytetrafluoroethylene (PTFE), have been utilized clinically for decades due to merits such as the excellent mechanical strength, tunable structure, and sufficient availability. The vascular prostheses are more acceptable by patients, as they can circumvent the additional surgical procedures and donor site morbidity by autologous vascular grafts [1,2]. Nevertheless, commercial PTFE grafts are only clinically successful as replacements of large-caliber vessels (>6 mm). In applications involving small-diameter vascular grafts, they generally suffer from the poor long-term patency rate and therefore fail to meet rigorous clinical requirements [1,3].

Luminal thrombosis and intimal hyperplasia are the main causes of poor long-term patency of prosthetic vascular grafts. Endothelialization of graft lumen is an effective strategy to prevent the luminal thrombosis and intimal hyperplasia of PTFE grafts [4–6] and the long-term patency can be significantly improved as a result. Since spontaneous endothelialization of pristine PTFE grafts is impossible *in vivo* [7], a tissue-engineered method by pre-seeding grafts with autologous endothelial cells has been proposed and is quite successful [8,9]. Nevertheless, its widespread clinical adoption is plagued by the high production cost, complicated procedures, and particularly the need for a lead time of up to

* Corresponding author.
** Corresponding author.
*** Corresponding author.
E-mail addresses: hy.wang1@siat.ac.cn (H. Wang), lp.tong@siat.ac.cn (L. Tong), paul.chu@cityu.edu.hk (P.K. Chu).

http://dx.doi.org/10.1016/j.biomaterials.2017.06.023
0142-9612/

several months [2,10]. In this respect, off-the-shelf grafts that facilitate rapid endothelialization *in situ* are highly desirable [11,12]. Circulating endothelial progenitor cells (EPCs), which can be mediated by various chemokines [13,14] including stromal cell-derived factor-1α (SDF-1α) [15,16], is essential to spontaneous endothelialization of prosthetic vascular grafts. By involving SDF-1α, prosthetic grafts can attain spontaneous endothelialization *via* recruitment of EPCs from the blood stream [17,18]. On the other hand, intimal hyperplasia, a result of the migration, over-proliferation, and matrix synthesis of native smooth muscle cells (SMCs), is provoked by mechanical stretching and chronic inflammatory response at the anastomotic site [19,20]. Immobilization of the transmembrane protein CD47 is another strategy to attenuate intimal hyperplasia [21,22], as the inflammatory response of prosthetic grafts can be effectively alleviated by the competence of CD47 as a "marker of self" [23]. In addition, luminal thrombosis can be ascribed to the intrinsic thrombogenicity of vascular prostheses and surface heparinization of prosthetic grafts has been proven successful in thrombus prevention [24,25].

Among the various techniques for surface modification of prosthetic grafts with biomolecules, covalent immobilization is a good choice on account of the long-term persistence of biomolecules after functionalization [26,27]. Nevertheless, owing to the prominent chemical inertness of PTFE, covalent modification of grafts by wet chemical methods is quite difficult. Alternatively, physical techniques such as plasma treatments have been demonstrated to alter the surface properties of biopolymers [28–31]. In particular, plasma immersion ion implantation (PIII) is a simple and effective technique to tailor the surface chemistry and topography of PTFE [32,33]. It is expected that covalent immobilization of biomolecules on PTFE is facilitated by PIII albeit in the absence of chemical cross-linkers [34,35].

In this study, PTFE which has undergone N_2 PIII is further functionalized by covalent immobilization of heparin, CD47, and/or SDF-1α, and the antithrombotic capability, endothelialization potential, as well as anti-inflammatory functions are investigated systematically. From the perspective of reduced thrombogenicity, rapid endothelialization, and low inflammatory immune response, PTFE after surface functionalization is promising enabling the development of small-diameter prosthetic vascular grafts with good long-term patency.

2. Materials and methods

2.1. Materials

The heparin sodium salt (from porcine intestinal mucosa, Grade I-A, ≥180 USP units/mg), toluidine blue O (TB), lipopolysaccharides (LPS, from *Escherichia coli*), AMD3100, thiazolyl blue tetrazolium bromide (MTT), horseradish peroxidase (HRP), paraformaldehyde (PFA), sodium dodecyl sulfate (SDS), Triton X-100, bovine serum albumin (BSA), and FITC labeled phalloidin were produced by Sigma-Aldrich, USA. The human TNF-α Valukine ELISA kit and human CXCL12/SDF-1α Quantikine ELISA kit were purchased from R&D systems, USA. The rabbit monoclonal vinculin antibody, Alexa Fluor 546 conjugated goat anti-rabbit IgG secondary antibody, fetal bovine serum (FBS), Dulbecco's modified eagle medium (DMEM), and RPMI 1640 medium were obtained from Life technologies, USA. The lactate dehydrogenase (LDH) assay kit, phorbol-12-myristate-13-acetate (PMA), 4′,6-diamidino-2-phenylindole dyes (DAPI) were obtained from Beyotime Biotechnology, China, and the recombinant human SDF-1α was obtained from Peprotech, USA. The recombinant human CD47 protein was acquired from Abcam, USA, and EGM-2 BulletKit was obtained from Lonza, Switzerland.

2.2. N_2 PIII treatment of PTFE

The PTFE sheets purchased from Goodfellow (0.25 mm in thickness) were cut into circular disks with a diameter of 15 mm. The substrates were ultrasonically cleaned in acetone, ethanol, and distilled water before inserting into the vacuum chamber of the gas PIII equipment. N_2 PIII was performed on the insulating PTFE samples according to procedures described previously [32]. Briefly, the PTFE samples were mounted on the sample stage which was connected to a negative high-voltage power supply. A stainless steel mesh placed 1 cm above the PTFE surface was electrically grounded to allow the plasma to diffuse through and be accelerated to the samples. High purity N_2 was introduced into the chamber to maintain a working pressure of 9.0×10^{-2} Pa. The N_2 plasma were generated by a radio frequency (RF) power of 1000 W and N_2 PIII was carried out for 3 h by applying a pulsed negative bias to the sample stage with the voltage of −15 kV, frequency of 500 Hz, and pulse duration of 20 μs.

2.3. Sample characterization

Scanning electron microscopy (SEM, JSM 7001F, JEOL, Japan) and atomic force microscopy (AFM, NanoScope V MultiMode system, Veeco, USA) were employed to evaluate the surface topography. The samples were dried and sputter-coated with gold prior to SEM observation and the surface roughness was determined by AFM. The static contact angles were measured with 5 μl of distilled water by the sessile drop method on the Rame'-Hart instrument (USA) under ambient conditions and X-ray photoelectron spectroscopy (XPS) was conducted on the Physical Electronics PHI 5802 (USA) equipped with a monochromatic Al K_α source.

2.4. Immobilization of biomolecules

The procedures for immobilization of heparin, CD47 and SDF-1α are schematically illustrated in Fig. 1. Briefly, the PTFE samples after undergoing N_2 PIII were degassed in the phosphate-buffered saline (PBS) solution and immersed in 500 μg/ml of the heparin solution or binary solution containing 500 μg/ml heparin and 1 μg/ml CD47 for 12 h at 4 °C. Afterwards, the samples were taken out, rinsed with PBS, and dipped into a 1 μg/ml SDF-1α solution for another 12 h at 4 °C. The above modified samples were designated as PTFE, N2, N2-Hep, N2-Hep-SDF, and N2-Hep-SDF-CD47, respectively.

2.5. Determination of heparin

The amount of immobilized heparin was determined by the modified TB method [36]. The TB solution was prepared by dissolving the TB reagent (0.005 w/v%) and NaCl (0.2 w/v%) in HCl (0.01 M). Using 24-well tissue culture plates as the holders, a series of 250 μl standard heparin solutions and various samples with 250 μl PBS solution were separately incubated with 250 μl of TB solution at room temperature for 30 min to allow the formation of TB-heparin complex. Subsequently, solutions were collected and mixed with 500 μl of n-hexane vigorously. The TB-heparin complex was extracted into the organic phase while the unreacted TB remained in the aqueous phase. 200 μl of the aqueous phase were transferred to a 96-well plate and the absorbance at 631 nm was monitored on a microplate spectrophotometer (Eon, Biotek, USA). According to the standard curve obtained with standard heparin solutions, the absolute amount of heparin immobilized on each sample was calculated.

To determine the shelf-life, the N2 samples were stored under ambient conditions for 72 and 198 days prior to heparin solution incubation and subsequent quantification of immobilized heparin.

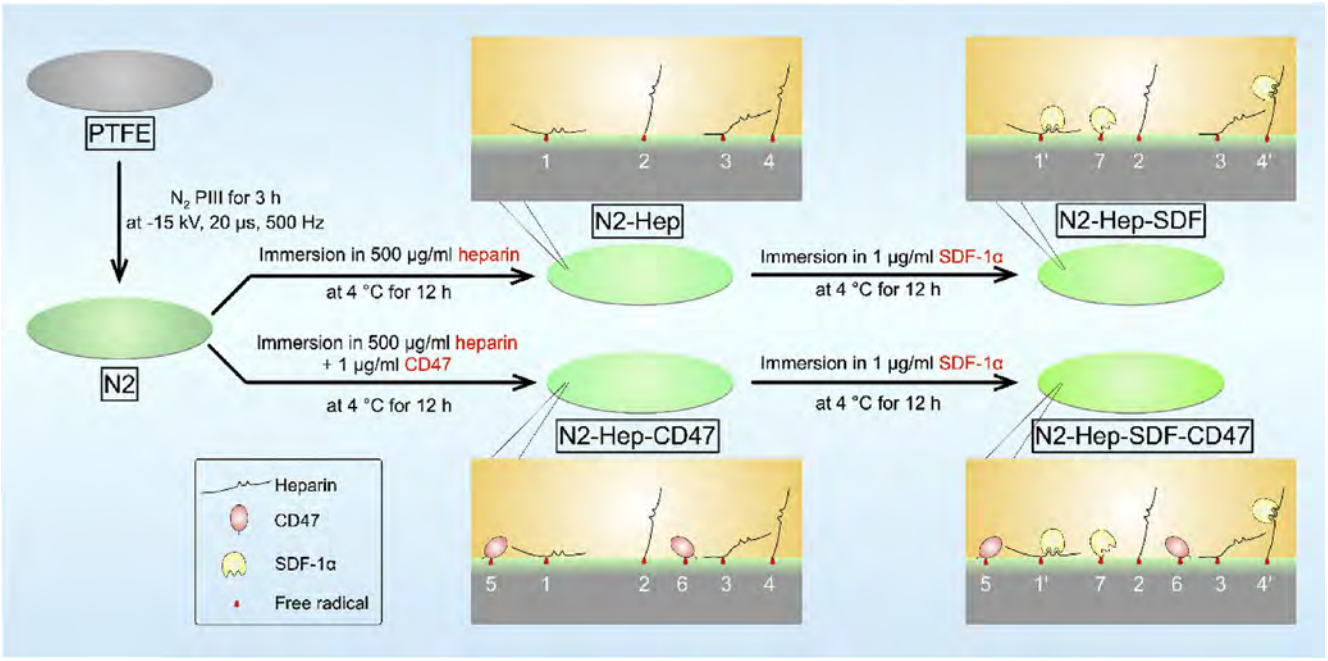

Fig. 1. Schematic illustration of the processing procedures and the corresponding sample designations. Note that all the biomolecules can be covalently immobilized by interacting with free radicals (binding 1–7) and SDF-1α is also conjugated to heparin by affinity binding (binding 1′ and 4′).

To assess the stability of heparin immobilized on the samples, the N2-Hep samples were immersed in PBS solution at 37 °C for 7, 14, and 28 days prior to heparin quantification.

2.6. Re-calcified whole blood clotting and platelet adhesion

The anticoagulant ability of samples was determined by a re-calcified whole blood clotting assay. With consent, fresh human whole blood was drawn from healthy adult volunteers according to ethics rules, maintained in the anticoagulant tubes, and used within 12 h after collection. After addition of 50 μl of the $CaCl_2$ solution (0.1 M), various samples were separately incubated with 500 μl of re-calcified whole blood at room temperature for 30 min. The clotted blood on each sample was rinsed with distilled water, blotted on a paper towel, and weighed.

The platelet-rich plasma was obtained by centrifuging the human whole blood at 200 g for 20 min 100 μl of the platelet-rich plasma were introduced onto each sample and incubated at 37 °C for 1 h. After gently rinsing the samples with PBS, the amount of platelets adhered on various samples was determined by a LDH assay according to manufacturer's instructions. The morphology of the platelets was examined by SEM.

2.7. Determination of SDF-1α and in vitro EPCs adhesion

The N2-Hep-SDF and N2-Hep-SDF-CD47 samples were incubated with PBS for 1, 3, and 5 days, and the released and immobilized SDF-1α was determined using a commercial ELISA kit according to the manufacturer's protocols (Supplementary information).

The circulating EPCs were isolated by adherence culture. Briefly, the human peripheral blood was collected from healthy adult volunteers after informed consent and added with heparin for anticoagulation. The collected blood was diluted 1:1 with PBS, overlaid onto a lymphocyte separation medium, and centrifuged at 1000 *g* for 15 min. Afterwards, the mononuclear cells were carefully isolated from the buffy coat, rinsed thrice with 2% FBS in PBS solution, resuspended in EGM-2 BulletKit, seeded onto the culture dishes pre-coated by 0.1 mg/ml poly-L-lysine, and cultured in a humidified atmosphere of 5% CO_2 at 37 °C. The culture medium was refreshed every 3 days when the non-adherent cells and debris were aspirated. The adherent cells were further examined for the EPCs phenotype (Supplementary information) and used $\leq$ 3 passages in following experiments.

To assess EPCs adhesion *in vitro*, the samples were blocked with 1% BSA solution for 1 h prior to cell seeding. The EPCs were resuspended in the serum-free medium and seeded onto the samples at a density of 5×10^4 cells per sample by using 24-well tissue culture plates as the holders. In parallel, EPCs were pre-treated with 5 μg/ml AMD3100 at 37 °C for 30 min before being seeded onto various samples. After incubation at 37 °C for 1 h, the cells on samples were rinsed with PBS solution, and fixed with 4% PFA, and the adherent EPCs were counted from 10 random fields at 100 × magnification after DAPI staining.

2.8. Cytocompatibility and endothelialization

The cytocompatibility and endothelialization of the samples were investigated by human umbilical vein endothelial cells (HUVECs, ATCC CRL-1730) with glucose DMEM supplemented with 10% FBS, 2 mM L-glutamine, 1% penicillin/streptomycin as the culture medium.

To analyze the formation of focal adhesion, HUVECs were seeded on the samples at a density of 1×10^4 cells per sample with 24-well tissue culture plates as the holders. The tissue culture plate (TCP) served as the positive control. After incubation for 24 h, the cells were rinsed thrice with PBS, fixed with 4% PFA for 10 min, permeabilized with 0.1% Triton X-100 for 10 min, and blocked with 1% BSA for 30 min. Subsequently, the samples were incubated with rabbit anti-Vinculin primary antibody for 1 h and Alexa Fluor 546 conjugated goat anti-rabbit IgG secondary antibody for another 1 h. Afterwards, the cytoskeletal actin filaments (F-actin) of the HUVECs was stained with FITC conjugated phalloidin for 1 h and the nuclei were stained by DAPI for 5 min. The samples were mounted on

slides and photographed by a confocal scanning microscope (DMI4000B, Leica, Germany).

To investigate cell proliferation, HUVECs were seeded onto the samples at a density of 5×10^4 cells per sample with 24-well tissue culture plates as the holders. After incubation for 1 and 3 days, the samples bearing cells were transferred to a new 24-well plate and analyzed by the MTT assay according to the manufacturer's instructions.

After incubation for 3 days, the samples with HUVECs were mounted in a custom-built parallel-plate flow chamber to evaluate the cell resistance to laminar shear stress (10 dynes/cm^2) for 1 h. The cells retained on the samples were rinsed with PBS, fixed with 4% PFA, and quantified based on 10 random fields at 100 × magnification after DAPI staining. The cell retention rate was determined by the following relationship: Cell retention rate = Number of cells resisted to fluid shear stress/Number of cells adhered on samples initially × 100%.

The migratory behavior of HUVECs on the samples were evaluated using a wound healing model. Briefly, a cell-free gap with a width of 500 μm was generated in the middle of the cell monolayer by removing the silicone insert mounted on each sample. After incubation for 12 and 24 h, the cells on samples were stained with FITC conjugated phalloidin and examined by fluorescent microscopy (Axio Observer Z1, Carl Zeiss, Germany). The area covered by cells was determined by WimScratch Image Analysis.

Nitric oxide (NO) secretion from the HUVECs on samples was determined by using a NO-specific fluorescent probe DAF-FM DA (3-Amino,4-aminomethyl-2′,7′-difluorescein, diacetate) [37]. DAF-FM DA could passively diffuse across the cellular membranes and be deacetylated by the intracellular esterases to be DAF-FM (4-amino-5-methylamino-2′,7′-difluorescein) and fluoresce. Since the fluorescence intensity of DAF-FM DA was linear with the intracellular NO concentration, NO production from the cells could be determined by flow cytometry after incubation with DAF-FM DA. To analyze NO secretion, the HUVECs were seeded on the samples and TCP positive control at a density of 5×10^4 cells per sample by using 24-well tissue culture plates as the holders. After incubation for 48 h, the cells on the samples were rinsed with PBS and incubated with 5 μM DAF-FM DA for 30 min at 37 °C in darkness. Subsequently, the cells were detached from samples with 0.125% trypsin-EDTA, fixed with 2% PFA, and then washed and resuspended in PBS solution for the flow cytometry analysis of over 10,000 cells.

2.9. Anti-inflammatory assays

The human monocytic leukemia cell line, THP-1 (ATCC TIB-202), was maintained in RPMI 1640 supplemented with 10% FBS, 2 mM L-glutamine and 1% penicillin/streptomycin, in a humidified atmosphere of 5% CO_2 at 37 °C. In the anti-inflammatory assays, THP-1 monocytes were seeded onto the samples at a density of 1×10^5 cells per sample by using 24-well tissue culture plates as the holders, and the cells were induced to differentiate into macrophages by incubation with 160 nM PMA for 48 h. Afterwards, the cells on the samples were rinsed thrice with PBS to remove the non-adherent cells and fixed with 4% PFA, and the adherent macrophages were quantified based on 10 random fields at 100 × magnification after DAPI staining. The macrophages on samples were also fixed with 4% PFA and stained with FITC conjugated phalloidin. The morphology was examined by fluorescent microscopy (Axio Observer Z1, Carl Zeiss, Germany). After culturing in the PMA-free medium for 6 h, the macrophages on samples were stimulated with 100 ng/ml LPS for 24 h and the supernatants were collected and frozen at −20 °C for further analysis. According to the manufacturer's protocols, the TNF-α level was determined using a commercial ELISA kit, and normalized to the number of adherent cells.

2.10. Statistical analysis

The results were presented as mean ± standard deviation. One-way ANOVA followed by Student-Newman-Keuls post hoc test was performed to determine the statistical significance. Difference at $^*p < 0.05$ was considered to be significant and that at $^{**}p < 0.01$ was considered to be highly significant.

3. Results

3.1. Surface characterization of PTFE after N_2 PIII

The insulating PTFE samples are subjected to N_2 PIII using a special mesh-assisted implantation configuration as described previously [32]. As shown in Fig. 2A, the surface morphology of pristine PTFE is generally flat, although some pores inherited from the raw materials can be observed by SEM. After N_2 PIII, quasi-ordered “protrusions and valleys” with a scale of hundreds of nanometers emerge. The morphological difference is also confirmed by AFM and Fig. 2B shows that the root-mean-square roughness increases drastically from 17.9 nm of the pristine PTFE to 134 nm after N_2 PIII. Correspondingly, the wettability of PTFE surface is altered from being hydrophobic originally (115 ± 3°) to nearly superhydrophobic (147 ± 3°) (Fig. 2C) after N_2 PIII. Fig. 2D presents the high-resolution C 1s and N 1s spectra of the pristine and N_2 PIII samples with peak deconvolution. The prominent C-F peak of the pristine PTFE decreases in intensity after N_2 PIII in association with the emergence of C—O/C—N and C═O/C═N bonds. The surface chemical alteration on the N_2 PIII treated samples is evident.

3.2. Heparin immobilization and antithrombogenic properties

After surface modification by N_2 PIII, the PTFE samples are incubated in a heparin solution or the binary solution of heparin and CD47, followed by incubation in an SDF-1α solution to immobilize the biomolecules, as shown in Fig. 1. Prior to functionalization, the amount of heparin on PTFE and N2 samples is determined by the TB assay [36]. As expected, the amount of heparin attached to the PTFE is negligible, whereas heparin is immobilized on N2 at a density of about 1 μg/cm^2 (Fig. 3A). More importantly, the robust immobilization of heparin on N2 is not compromised even after long-term storage (up to 198 days) under ambient conditions (Fig. 3A). The stability of the heparin-loaded N2 is also evaluated under physiological conditions and *in vitro* measurements do not reveal any sign of heparin detachment for over 28 days (Fig. 3B).

Before and after multi-functionalization, the samples are incubated with re-calcified whole blood for 30 min to evaluate the anticoagulant activity by weighing the blood clot formed on the surface. As shown in Fig. 3C, N2 appear to activate blood coagulation to a much higher extent than PTFE, which is undesirable for employment as vascular materials. Fortunately, this drawback is circumvented by subsequent loading of heparin, as there is no significant difference in blood clotting between PTFE and the samples loaded with heparin. In the next step, the samples after incubation with the platelet-rich plasma are examined with respect to adherent platelets using the LDH assay (Fig. 3D) and SEM (Fig. S1). Different from the pristine PTFE samples showing abundant platelets adhering to the surface with an activated morphology and many typical pseudopods, all four kinds of N2-modified substrates show suppressed platelets adhesion and most of the adhered platelets maintain a spheroid shape without activation.

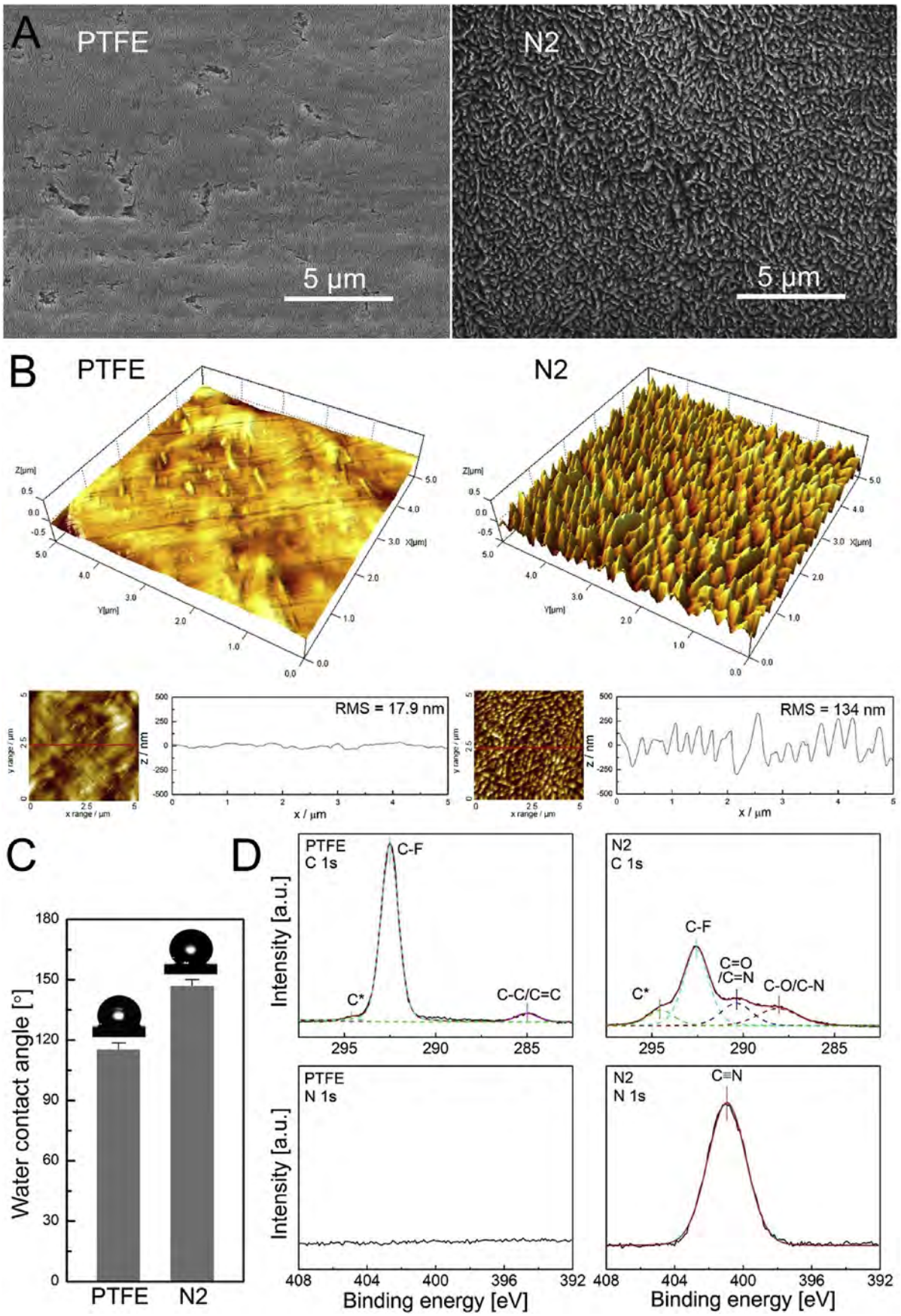

Fig. 2. Surface characterization of pristine PTFE (PTFE) and PTFE after N_2 PIII treatment (N2): (A) SEM images; (B) Three-dimensional AFM images and the corresponding cross-sectional height profiles along the red lines (RMS = root mean square); (C) Static water contact angles; (D) High resolution C 1s and N 1s spectra obtained by XPS. (For interpretation of the references to colour in this figure legend, the reader is referred to the web version of this article.)

3.3. SDF-1α functionalization and EPCs recruitment

The N2-Hep-SDF and N2-Hep-SDF-CD47 samples are further analyzed for the released and residual amount of SDF-1α by incubating them in the PBS solution at 37 °C for 1, 3, and 5 days. As shown in Fig. 4A, the loaded SDF-1α is released gradually with time but does not reach the plateau within 5 days of PBS incubation. The presence of CD47 on the samples has little influence on the release behavior of SDF-1α. Moreover, the residual amount of SDF-1α on the samples (Fig. 4B) is orders of magnitude larger than the released amount and no obvious loss of SDF-1α is observed for an incubation time of up to 5 days.

As aforementioned, immobilization of SDF-1α probably leads to spontaneous endothelialization of the surface by recruiting circulating EPCs from the blood stream. To demonstrate the specific recognition effect between the SDF-loaded samples and circulating EPCs, EPCs are first isolated from human peripheral blood by adherence culture for 7 days and then identified for the specific surface markers such as CD34, CD133, Flk-1, and SDF-1α specific receptor CXCR4 (Fig. S2) [38]. Fig. 4C and Fig. S3 confirm the capability of immobilized SDF-1α to enhance receptor-mediated attachment of EPCs. In particular, significantly more EPCs are attracted by the SDF-1α-loaded samples than the SDF-1α free ones. When EPCs are pre-incubated with the CXCR4 specific antagonist AMD3100, pro-adhesion on the SDF-1α-loaded samples is greatly attenuated, thereby corroborating the specific recognition between SDF-1α and CXCR4 receptor of EPCs.

3.4. Cytocompatibility and endothelialization

The modified samples are cultured with HUVECs and cytocompatibility is assessed by focal adhesion, cell proliferation, cell resistance to fluid shear stress, cell migration, and NO production by HUVECs. Formation of focal adhesion on the samples is examined by vinculin and F-actin immunostaining after HUVECs culture for 24 h. As shown in Fig. 5A, HUVECs on PTFE show a rounded morphology and a lack of stress fibers. In contrast, the cells spread well on the modified samples as well as positive control. A dense network of F-actin and punctate distribution of vinculin are observed throughout the cell body, indicating ongoing vinculin localization to the ends of stress fibers to form focal adhesion.

After HUVECs culturing for 1 and 3 days, cell proliferation is evaluated by the MTT assay. Fig. 5B reveals that HUVECs proliferation on N2 is much better than that on PTFE, while the load of heparin further enhances cell proliferation. Nonetheless, all the modified samples are inferior to the positive control with regard to HUVECs proliferation. After 3 days, the seeded HUVECs are able to reach a confluent monolayer on the samples except PTFE (Fig. S4). The cells on the samples are further introduced into a parallel-plate flow chamber and exposed to shear stress for 1 h. As shown in Fig. 5C, only a few cells on the modified samples are detached, whereas less than half of the cells on PTFE are retained. To investigate the migratory behavior of HUVECs on various samples by wound healing assay, a cell-free gap of 500 μm is generated by removal of the culture insert. It is obvious that the exposed gap can be gradually closed on account of directional cell migration (Fig. 5D). The quantitative results (percentage of cell-covered area) in Fig. 5D demonstrate the non-significant difference between the modified samples and positive control (Fig. S5). In contrast, the results for PTFE are null since the cells on PTFE cannot reach confluence. NO is an important signaling molecule that plays a multifunctional role in cardiovascular physiology [39]. Flow cytometry shows that the HUVECs cultured on N2, N2-Hep, N2-Hep-SDF, and N2-Hep-SDF-CD47 have a higher percentage of NO-

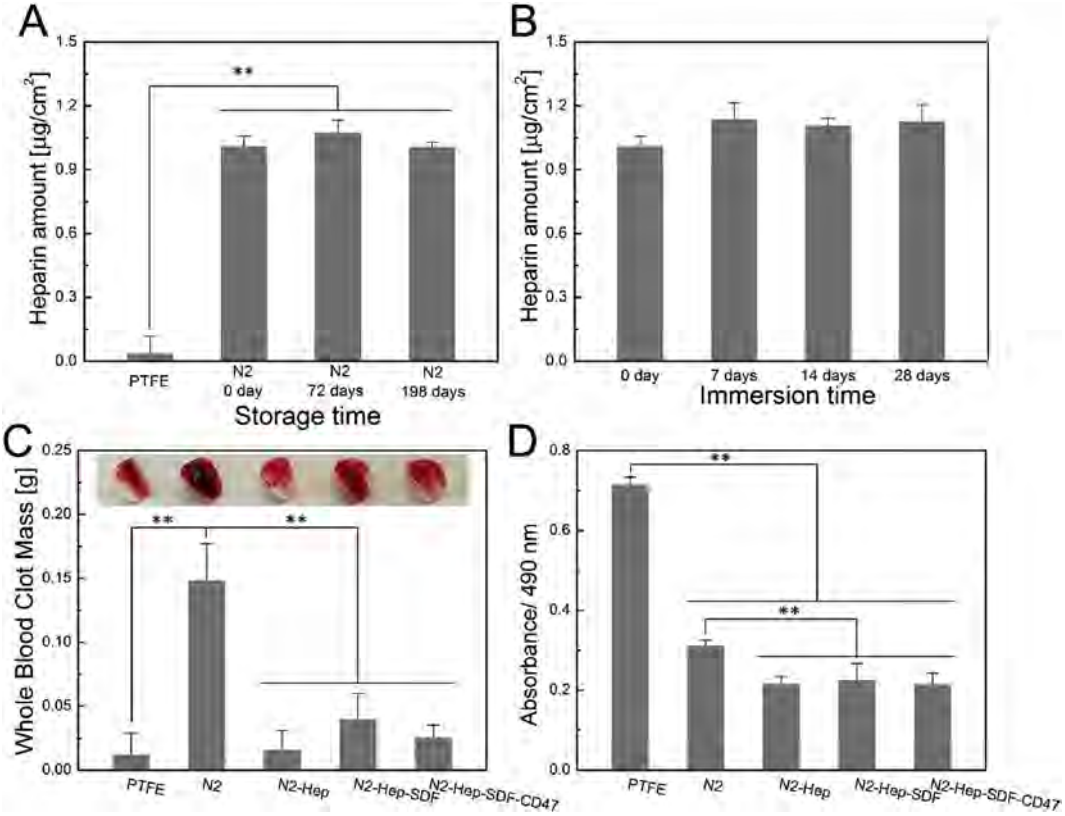

Fig. 3. Heparin immobilization and antithrombotic effects: (A) Heparin loading capability of pristine PTFE, and the N2 samples after being stored under ambient conditions for 0, 72, and 198 days; (B) Heparin amounts on the N2-Hep samples after incubation in PBS for 0, 7, 14, and 28 days; (C) Mass of blood clot formed on each sample after incubating with re-calcified whole blood for 30 min. The corresponding photograph is inseted; (D) Relative amount of adherent platelets on each sample after incubation with PRP for 1 h.

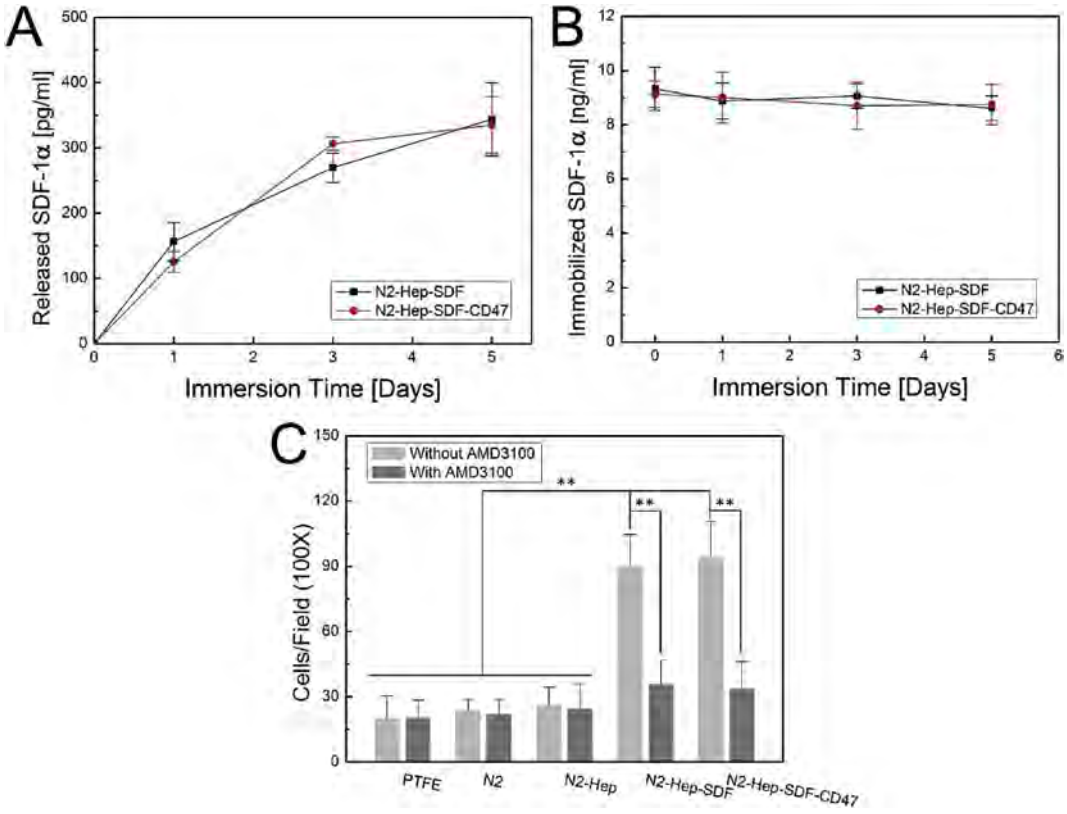

Fig. 4. SDF-1α functionalization and EPCs recruitment: (A) Cumulative release of SDF-1α from the samples bearing SDF-1α after incubation in PBS for 1, 3, and 5 days; (B) Amounts of SDF-1α retained on the samples after incubation in PBS for 1, 3, and 5 days; (C) Amounts of EPCs adhering on each sample before and after the treatment with AMD3100.

positive cells than those on PTFE and positive control (Fig. S6). Evidently, the endothelial functions of PTFE are significantly improved after N_2 PIII and functionalization with biomolecules.

3.5. CD47 loading and anti-inflammatory effects

Besides HUVECs assessments, THP-1 cells are employed to investigate the immune response of monocytes-macrophages to the samples [40]. After the THP-1 cells on samples are induced into macrophage by treatment of PMA, the macrophage-like phenotypes such as cell adhesion, cell morphology, and TNF-α secretion of cells in response to LPS stimulation are analyzed. The pristine PTFE is more favorable than the modified samples with respect to the adhesion of THP-1 derived macrophages (Fig. 6A and B). The adherent cells on PTFE are in the activated state. They not only show an irregular morphology, but also are abundant with filopodia (blue arrow) at the periphery and podosomes (red arrows) throughout the cell body (Fig. 6C). In contrast, fewer THP-1 derived macrophages adhere onto the N2-modified samples and most of them are inactivated. Further reduction in adherent cells is observed from N2-Hep-SDF-CD47 and N2-CD47 (N2 sample functionalized with CD47 solely), disclosing the anti-inflammatory effect rendered by immobilized CD47. With regard to secretion of pro-inflammatory cytokine TNF-α by THP-1 derived macrophages, Fig. 6D confirms the anti-inflammatory functions of all the modified samples, especially the two kinds of samples bearing CD47.

4. Discussion

Plasma techniques are widely used in surface modification and PIII with unique advantages such as non-line-of-sight processing and ion mixing is especially attractive to biomedical implants. During PIII, energetic ions are implanted into the PTFE substrate by the electric field and stopped in the substrate *via* nuclear stopping and electronic stopping. Nuclear stopping damages the PTFE partially mainly in the form of chain scission. On the atomic scale, the C-F bonds in PTFE are broken, accompanied with an obvious increase of the end groups (C* shown in Fig. 2D). Concerning the microscopic morphology, the incident ions erode the PTFE to create a rough surface structure with protrusions and valleys (Fig. 2A and B).

Electronic stopping forms free radicals which may cause either polymer chain cross-linking or surface reactions with outside species. The high reactivity of free radicals is responsible for the emergence of various oxygen- and nitrogen-containing groups on the samples after N_2 PIII. In general, although polar groups on the surface normally enhance the hydrophilicity, the N2 samples are found to be superhydrophobic (Fig. 2C). It is believed to be the "lotus effect" stemming from the surface nanostructures [41]. For demonstration, after the PTFE samples are exposed to the N_2 plasma for 3 h (without bias) to perform simple chemical modification, a water contact angle of $50 \pm 3^\circ$ is observed, thus revealing the hydrophilic nature of the oxygen- and nitrogen-containing groups. The free radicals generated by gas PIII have been proven to be long-lived and mobile [34] and the ion-implanted region underneath the surface can serve as a reservoir of abundant free radicals. Since the free radicals are very reactive and migrate randomly, most of them are finally quenched in the bulk of the samples. However, a substantial amount of the free radicals can continuously migrate to the sample surface without being quenched and react with environmental molecules covalently.

By taking advantage of this unique mechanism, the samples

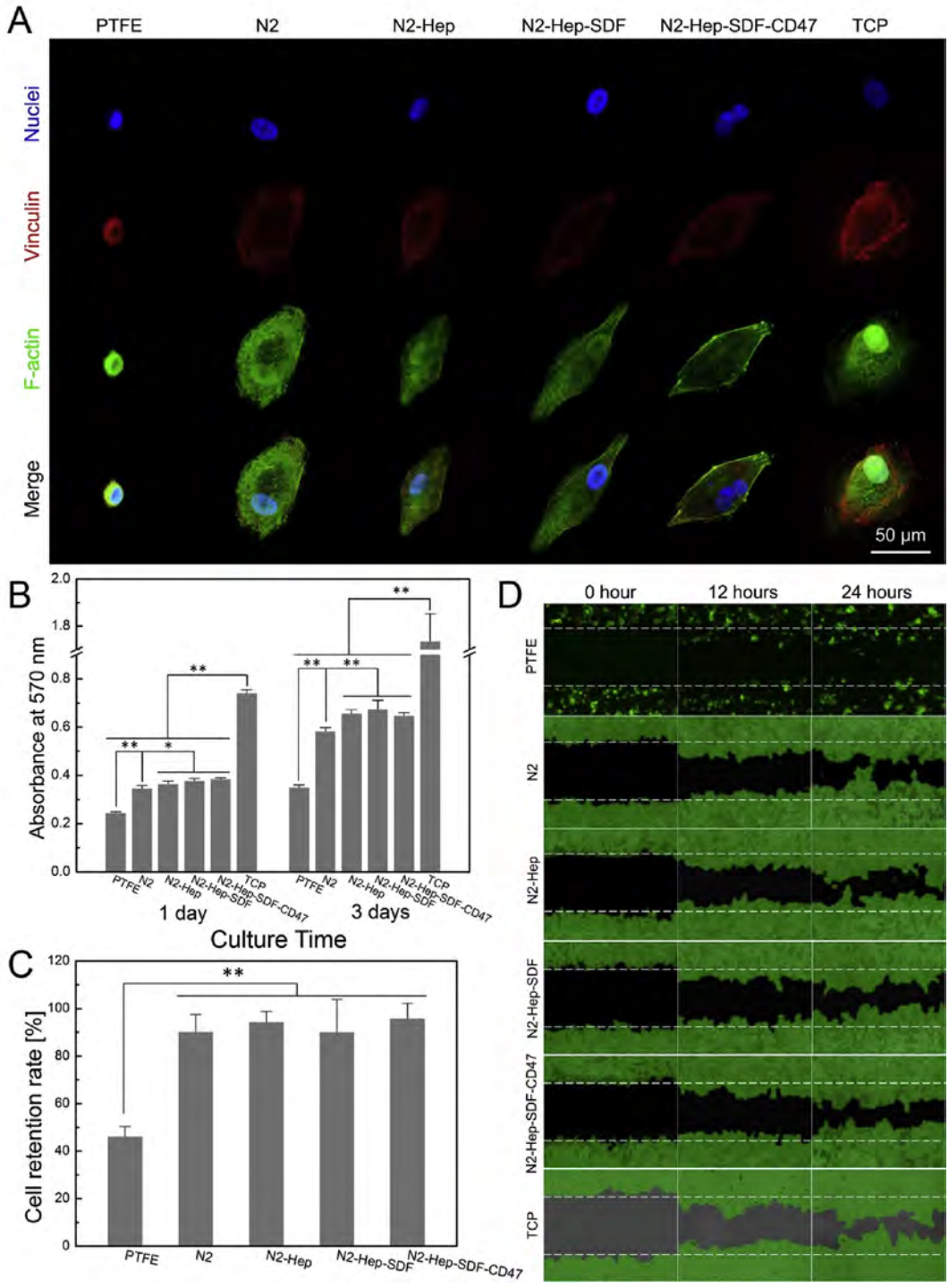

Fig. 5. Cytocompatibility and endothelialization: (A) Representative confocal images of HUVECs after incubating the cells on each sample and TCP positive control for 24 h. Note the focal adhesion (red) and cytoskeleton organization (green) of adherent cells; (B) Proliferation of HUVECs on each sample and TCP positive control after incubation for 3 days; C) Cell retention rate of the HUVECs monolayer on each sample and TCP positive control after introducing the samples bearing cells into a parallel-plate flow chamber and exposure to shear stress (10 dynes/cm^2) for 1 h; (D) Migration of HUVECs on each sample and TCP positive control into the cell-free gap zone (500 μm in width) after incubation for 0, 12, and 24 h. (For interpretation of the references to colour in this figure legend, the reader is referred to the web version of this article.)

after N_2 PIII can link to various biomolecules in the surrounding solution even in the absence of chemical linkers. It is well known that proteins tend to adhere to hydrophobic samples such as pristine PTFE on account of the hydrophobic interaction. However, the supplementary results in Fig. S7 demonstrate that the HRP physically absorbed on pristine PTFE can be easily removed by SDS, a potent ionic surfactant capable of disrupting non-covalent interactions, whereas the proteins immobilized on the N2 samples are resistant to SDS elution. The bioactive conformation of HRP can be well-preserved after covalent immobilization. Unlike proteins, heparin is a kind of glycosaminoglycan with good hydrophilicity and barely adsorbs onto pristine PTFE. After creation of free radicals

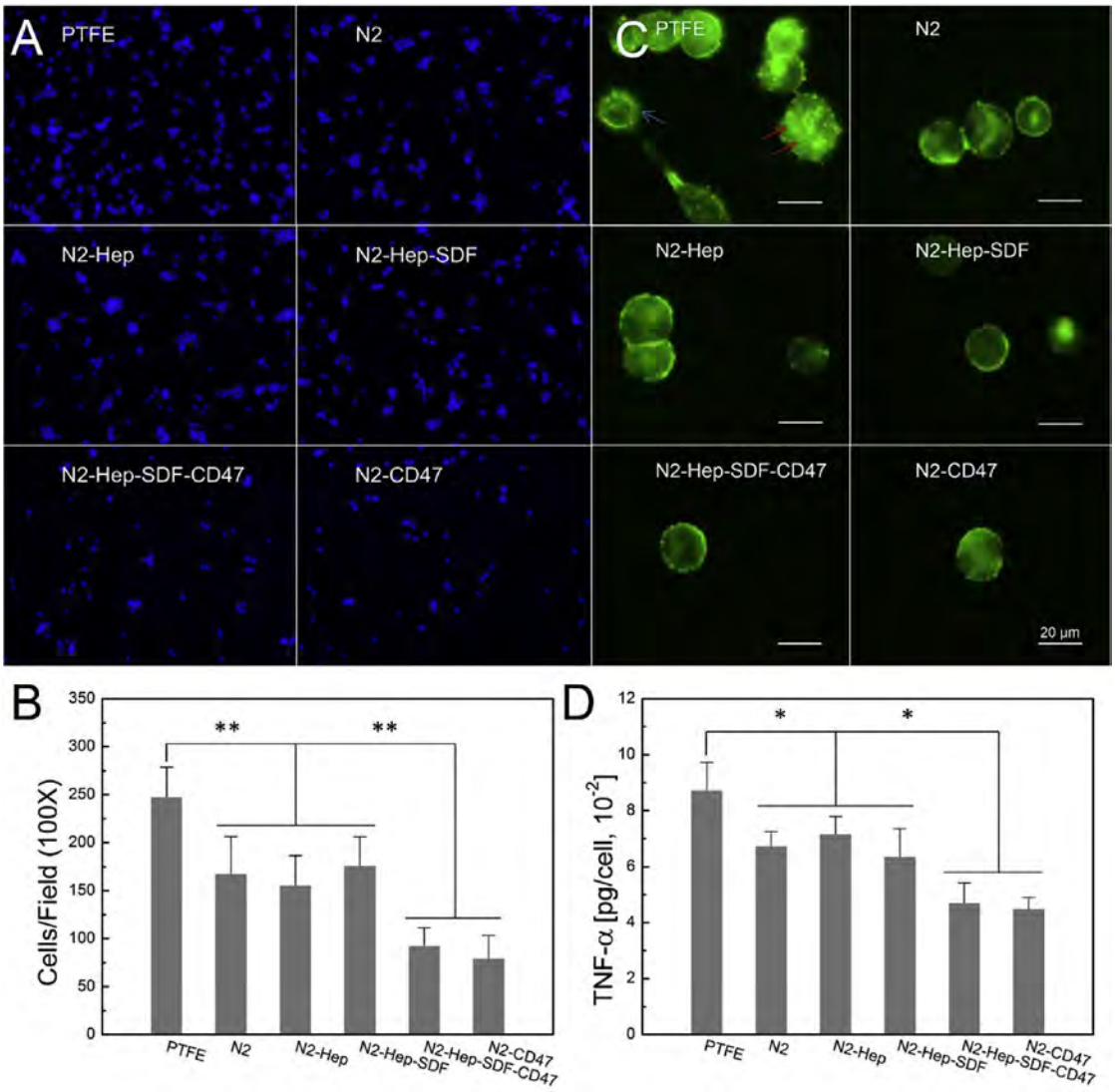

Fig. 6. CD47 loading and anti-inflammatory effects: (A) Representative fluorescent images of differentiated THP-1 cells on each sample after 160 nM PMA incubation for 48 h; (B) Corresponding amount of differentiated THP-1 cells on each sample; (C) Morphology of differentiated THP-1 cells on each sample. Note the filopodia (blue arrow) and podosomes (red arrows) of the cells on PTFE; (D) TNF-α secretion level of differentiated THP-1 cells on each sample after 100 ng/ml LPS stimulation for 24 h. (For interpretation of the references to colour in this figure legend, the reader is referred to the web version of this article.)

by N_2 PIII, the surface of the N2 samples is energetic enough for heparin grafting (Fig. 3A) and the loaded amount of heparin is almost unchanged after incubation in PBS for up to 28 days (Fig. 3B). The high stability of immobilized heparin on N2 can be ascribed to the covalent interaction. In addition, incubation in the binary solution provides the feasibility of simultaneous immobilization. According to our preliminary experiments on N2 samples loaded with heparin and/or HRP, there is no significant change in the loaded amounts among samples incubated in 500 μg/ml heparin, 50 μg/ml HRP, and binary solution of heparin + HRP (data not shown). Moreover, the N2 samples have a long shelf-life, as demonstrated by their effectiveness in binding biomolecules (Fig. 3A and Fig. S7) after over 6 months of storage under ambient conditions.

According to our preliminary studies, the N2 samples are further functionalized with heparin, CD47, and/or SDF-1α to evaluate potential cardiovascular applications. As shown in Fig. 1, the N2 samples are incubated in heparin or heparin/CD47 binary solution to immobilize the biomolecules. During the incubation processes, heparin and/or CD47 in the solution react with free radicals and can be covalently grafted (binding 1, 2, 3, and 4 for heparin, and binding 5 and 6 for CD47). Thereafter, the samples are transferred to the SDF-1α solution for further functionalization. On account of the high affinity between SDF-1α and heparin, SDF-1α can conjugate to the immobilized heparin (binding 1′ and 4′) besides direct grafting on samples (binding 7). In comparison, only a few of the surface-grafted heparin molecules are bound with SDF-1α due to their enormous difference in concentration.

Heparin is the most commonly used anticoagulant clinically and surface heparinization has been proven as an efficient strategy to prevent thrombus formation on blood contacting biomaterials [24]. Although the N2 samples appear to be procoagulant, further decoration with heparin can overcome this disadvantage (Fig. 3C), indicating that the antithrombogenic function of heparin is retained after covalent immobilization [42]. Owing to the high affinity between heparin and SDF-1α [25], the immobilized heparin can serve as a localized delivery platform for the storage and sustained release of SDF-1α (Fig. 4A). On the other hand, immobilization of heparin on the samples enhances HUVECs proliferation slightly (Fig. 5B) [43]. Both the LDH assay (Fig. 3D) and SEM (Fig. S1)

reveal significantly fewer platelets on the N2 samples, and the amounts of adherent platelets on samples can be further reduced after surface heparinization. It is believed that suppression of platelet adhesion originates from the cooperative effect of the hydrophilic surface [44] and nanotopography [45] on the samples, in addition to the antithrombogenic function of immobilized heparin [42].

Although early thrombus formation on the PTFE grafts can be efficiently inhibited by heparin immobilization, it is imperative to line them with endothelium for the achievement of long-term patency. Generally, there are two main reasons for the lack of endothelialization capability on PTFE grafts. The first reason is that the *trans*-anastomotic migration of endothelial cells is insufficient [7]. Clinical data show that the endothelial coverage of prosthetic grafts is limited to the peri-anastomotic region (1–2 cm) even after years of implantation. To solve this problem, the strategy about *in situ* endothelialization *via* recruitment of endogenous progenitor cells has been proposed [17]. In this study, SDF-1α is used for the surface functionalization of PTFE. SDF-1α is a potent chemokine which can specially recognize the CXCR4 receptor of circulating EPCs (Fig. S2). Immobilization of SDF-1α is effective in capturing EPCs under flowing conditions [46–49]. As shown in Fig. 4C and Fig. S3, the presence of SDF-1α on the samples greatly enhances adhesion of EPCs, whereas this enhancement can be precluded by blocking the CXCR4 receptor of EPCs with AMD3100. Another reason for insufficient endothelialization is the inherent bioinertness of PTFE. If the sample surface does not support cell survival, the benefit to EPCs recruitment is meaningless. It has been demonstrated that the surface properties of PTFE substrate can be readily altered by gas PIII [32,33]. N_2 PIII can overcome the bioinertness of PTFE so that surface functionalization with biomolecules can be facilitated. After the dual process, the cellular functions of HUVECs on the samples such as formation of focal adhesion, cell proliferation, cell resistance to fluid shear stress, and cell migration are improved (Fig. 5A–D). The cells on the modified samples are even better than those on pristine PTFE and TCP from the perspective of cellular production of NO signaling molecules for better endothelial functions (Fig. S6).

Intimal hyperplasia is another major challenge against the long-term patency of prosthetic vascular grafts. It is well known that graft implantation is normally accompanied by a cascade of foreign body reactions including recruitment of monocytes, differentiation of monocytes into macrophages, and secretion of inflammatory cytokines [50]. In response to inflammatory stimuli, vascular smooth muscle cells can over-proliferate leading to the intimal thickening and gradual reduction in patency [20]. It has been documented that CD47 is a “marker of self” and its employment can attenuate the intimal hyperplasia of prosthetic grafts by modulating the host immune response [51–53]. By taking advantage of the “incubation for immobilization” method to grafting CD47, the immune response of monocytes-macrophages can be effectively inhibited (Fig. 6).

5. Conclusion

A synergetic approach is proposed to tailor the surface properties of PTFE for better cardiovascular applications. Initial N_2 PIII changes the surface chemistry and topography of PTFE giving rise to the formation of free radicals which enable covalent binding with biomolecules without using chemical linkers. After N_2 PIII, grafting with heparin, SDF-1α, and CD47 is performed to endow PTFE with multi-biofunctions including antithrombosis, EPCs recruitment, rapid endothelialization, and anti-inflammation. The surface-functionalized PTFE has large potential in the development of off-the-shelf vascular grafts with good long-term patency. This versatile strategy can also be extended to grafting of other functional biomolecules on polymeric substrates to expand their roles in biomedical applications.

Acknowledgements

The authors acknowledge financial support from National Natural Science Foundation of China (NSFC) (Nos. 31470044 and 51503220), Shenzhen Science and Technology Research Funding (Nos. JCYJ20150401145529017, and JSGG20160229195900623), Leading Talents of Guangdong Province Program (No. 00201520), Shenzhen Peacock Program (No. KQTD2016030111500545), Hong Kong Research Grants Council (RGC) General Research Funds (GRF) (No. CityU 11301215), and City University of Hong Kong Strategic Research Grant (SRG) (No. 7004644).

Appendix A. Supplementary data

Supplementary data related to this article can be found at http://dx.doi.org/10.1016/j.biomaterials.2017.06.023.

References

[1] R.Y. Kannan, H.J. Salacinski, P.E. Butler, G. Hamilton, A.M. Seifalian, Current status of prosthetic bypass grafts: a review, J. Biomed. Mater. Res. Part B 74 (1) (2005) 570–581.
[2] D.G. Seifu, A. Purnama, K. Mequanint, D. Mantovani, Small-diameter vascular tissue engineering, Nat. Rev. Cardiol. 10 (7) (2013) 410–421.
[3] P. Klinkert, P.N. Post, P.J. Breslau, J.H. van Bockel, Saphenous vein versus PTFE for above-knee femoropopliteal bypass. A review of the literature, Eur. J. Vasc. Endovasc. Surg. 27 (4) (2004) 357–362.
[4] C. Michiels, Endothelial cell functions, J. Cell. Physiol. 196 (3) (2003) 430–443.
[5] N. Kipshidze, G. Dangas, M. Tsapenko, J. Moses, M.B. Leon, M. Kutryk, P. Serruys, Role of the endothelium in modulating neointimal formation: vasculoprotective approaches to attenuate restenosis after percutaneous coronary interventions, J. Am. Coll. Cardiol. 44 (4) (2004) 733–739.
[6] T. Liu, S. Liu, K. Zhang, J. Chen, N. Huang, Endothelialization of implanted cardiovascular biomaterial surfaces: the development from in vitro to in vivo, J. Biomed. Mater. Res. Part A 102 (10) (2014) 3754–3772.
[7] P. Zilla, D. Bezuidenhout, P. Human, Prosthetic vascular grafts: wrong models, wrong questions and no healing, Biomaterials 28 (34) (2007) 5009–5027.
[8] J.T. Krawiec, D.A. Vorp, Adult stem cell-based tissue engineered blood vessels: a review, Biomaterials 33 (12) (2012) 3388–3400.
[9] L. Bordenave, P. Menu, C. Baquey, Developments towards tissue-engineered, small-diameter arterial substitutes, Expert Rev. Med. Dev. 5 (3) (2008) 337–347.
[10] N. L'Heureux, N. Dusserre, A. Marini, S. Garrido, L. de la Fuente, T. McAllister, Technology insight: the evolution of tissue-engineered vascular grafts-from research to clinical practice, Nat. Clin. Pract. Cardiovasc. Med. 4 (7) (2007) 389–395.
[11] A. de Mel, G. Jell, M.M. Stevens, A.M. Seifalian, Biofunctionalization of biomaterials for accelerated in situ endothelialization: a review, Biomacromolecules 9 (11) (2008) 2969–2979.
[12] S.L. Dahl, J.L. Blum, L.E. Niklason, Bioengineered vascular grafts: can we make them off-the-shelf? Trends Cardiovasc. Med. 21 (3) (2011) 83–89.
[13] A. Zampetaki, J.P. Kirton, Q. Xu, Vascular repair by endothelial progenitor cells, Cardiovasc. Res. 78 (3) (2008) 413–421.
[14] E. Chavakis, C. Urbich, S. Dimmeler, Homing and engraftment of progenitor cells: a prerequisite for cell therapy, J. Mol. Cell. Cardiol. 45 (4) (2008) 514–522.
[15] K. Stellos, M. Gawaz, Platelets and stromal cell-derived factor-1 in progenitor cell recruitment, Semin. Thromb. Hemost. 33 (2) (2007) 159–164.
[16] D.J. Ceradini, A.R. Kulkarni, M.J. Callaghan, O.M. Tepper, N. Bastidas, M.E. Kleinman, J.M. Capla, R.D. Galiano, J.P. Levine, G.C. Gurtner, Progenitor cell trafficking is regulated by hypoxic gradients through HIF-1 induction of SDF-1, Nat. Med. 10 (8) (2004) 858–864.
[17] M. Avci-Adali, G. Ziemer, H.P. Wendel, Induction of EPC homing on biofunctionalized vascular grafts for rapid in vivo self-endothelialization-a review of current strategies, Biotechnol. Adv. 28 (1) (2010) 119–129.
[18] D.E. Muylaert, J.O. Fledderus, C.V. Bouten, P.Y. Dankers, M.C. Verhaar, Combining tissue repair and tissue engineering; bioactivating implantable cell-free vascular scaffolds, Heart 100 (23) (2014) 1825–1830.
[19] M.S. Lemson, J.H. Tordoir, M.J. Daemen, P.J. Kitslaar, Intimal hyperplasia in vascular grafts, Eur. J. Vasc. Endovasc. Surg. 19 (4) (2000) 336–350.
[20] A.K. Mitra, D.M. Gangahar, D.K. Agrawal, Cellular, molecular and immunological mechanisms in the pathophysiology of vein graft intimal hyperplasia, Immunol. Cell Biol. 84 (2) (2006) 115–124.
[21] Y.K. Kim, E.Y. Chen, W.F. Liu, Biomolecular strategies to modulate the

macrophage response to implanted materials, J. Mater. Chem. B 4 (9) (2016) 1600–1609.
[22] T. Inoue, K. Croce, T. Morooka, M. Sakuma, K. Node, D.I. Simon, Vascular inflammation and repair: implications for re-endothelialization, restenosis, and stent thrombosis, JACC Cardiovasc. Interv. 4 (10) (2011) 1057–1066.
[23] P.A. Oldenborg, A. Zheleznyak, Y.F. Fang, C.F. Lagenaur, H.D. Gresham, F.P. Lindberg, Role of CD47 as a marker of self on red blood cells, Science 288 (5473) (2000) 2051–2054.
[24] S. Murugesan, J. Xie, R.J. Linhardt, Immobilization of heparin: approaches and applications, Curr. Top. Med. Chem. 8 (2) (2008) 80–100.
[25] I. Capila, R.J. Linhardt, Heparin-protein interactions, Angew. Chem. Int. Ed. Engl. 41 (3) (2002) 391–412.
[26] J.M. Goddard, J.H. Hotchkiss, Polymer surface modification for the attachment of bioactive compounds, Prog. Polym. Sci. 32 (7) (2007) 698–725.
[27] K.S. Masters, Covalent growth factor immobilization strategies for tissue repair and regeneration, Macromol. Biosci. 11 (9) (2011) 1149–1163.
[28] P. Slepicka, N.S. Kasalkova, J. Siegel, Z. Kolska, L. Bacakova, V. Svorcik, Nano-structured and functionalized surfaces for cytocompatibility improvement and bactericidal action, Biotechnol. Adv. 33 (6) (2015) 1120–1129.
[29] Z. Kolská, A. Řezníčková, M. Nagyová, N.S. Kasálková, P. Sajdl, P. Slepička, V. Švorčík, Plasma activated polymers grafted with cysteamine improving surfaces cytocompatibility, Polym. Degrad. Stab. (2014) 1011–1019.
[30] P. Slepička, L. Peterková, S. Rimpelová, A. Pinkner, N.S. Kasálková, Z. Kolská, T. Ruml, V. Švorčík, Plasma activated perfluoroethylenepropylene for cytocompatibility enhancement, Polym. Degrad. Stab. (2016) 130277–130287.
[31] I. Michaljaničová, P. Slepička, J. Hadravová, S. Rimpelová, T. Ruml, P. Malinský, M. Veselý, V. Švorčík, High power plasma as an efficient tool for polymethylpentene cytocompatibility enhancement, RSC Adv. 6 (79) (2016) 76000–76010.
[32] H. Wang, D.T. Kwok, M. Xu, H. Shi, Z. Wu, W. Zhang, P.K. Chu, Tailoring of mesenchymal stem cells behavior on plasma-modified polytetrafluoroethylene, Adv. Mater. 24 (25) (2012) 3315–3324.
[33] H. Wang, D.T. Kwok, W. Wang, Z. Wu, L. Tong, Y. Zhang, P.K. Chu, Osteoblast behavior on polytetrafluoroethylene modified by long pulse, high frequency oxygen plasma immersion ion implantation, Biomaterials 31 (3) (2010) 413–419.
[34] M.M. Bilek, D.V. Bax, A. Kondyurin, Y. Yin, N.J. Nosworthy, K. Fisher, A. Waterhouse, A.S. Weiss, C.G. dos Remedios, D.R. McKenzie, Free radical functionalization of surfaces to prevent adverse responses to biomedical devices, Proc. Natl. Acad. Sci. U. S. A. 108 (35) (2011) 14405–14410.
[35] S.G. Wise, A. Waterhouse, A. Kondyurin, M.M. Bilek, A.S. Weiss, Plasma-based biofunctionalization of vascular implants, Nanomedicine 7 (12) (2012) 1907–1916.
[36] I.K. Kang, O.H. Kwon, Y.M. Lee, Y.K. Sung, Preparation and surface characterization of functional group-grafted and heparin-immobilized polyurethanes by plasma glow discharge, Biomaterials 17 (8) (1996) 841–847.
[37] Y. Itoh, F.H. Ma, H. Hoshi, M. Oka, K. Noda, Y. Ukai, H. Kojima, T. Nagano, N. Toda, Determination and bioimaging method for nitric oxide in biological specimens by diaminofluorescein fluorometry, Anal. Biochem. 287 (2) (2000) 203–209.
[38] G.P. Fadini, D. Losordo, S. Dimmeler, Critical reevaluation of endothelial progenitor cell phenotypes for therapeutic and diagnostic use, Circ. Res. 110 (4) (2012) 624–637.
[39] A. de Mel, F. Murad, A.M. Seifalian, Nitric oxide: a guardian for vascular grafts? Chem. Rev. 111 (9) (2011) 5742–5767.
[40] W. Chanput, J.J. Mes, H.J. Wichers, THP-1 cell line: an in vitro cell model for immune modulation approach, Int. Immunopharm. 23 (1) (2014) 37–45.
[41] A. Marmur, The lotus effect: superhydrophobicity and metastability, Langmuir 20 (9) (2004) 3517–3519.
[42] X.L. Liu, L. Yuan, D. Li, Z.C. Tang, Y.W. Wang, G.J. Chen, H. Chen, J.L. Brash, Blood compatible materials: state of the art, J. Mater. Chem. B 2 (35) (2014) 5718–5738.
[43] R. Sasisekharan, Z. Shriver, G. Venkataraman, U. Narayanasami, Roles of heparan-sulphate glycosaminoglycans in cancer, Nat. Rev. Cancer 2 (7) (2002) 521–528.
[44] B. Sivaraman, R.A. Latour, The relationship between platelet adhesion on surfaces and the structure versus the amount of adsorbed fibrinogen, Biomaterials 31 (5) (2010) 832–839.
[45] L. Chen, D. Han, L. Jiang, On improving blood compatibility: from bioinspired to synthetic design and fabrication of biointerfacial topography at micro/nano scales, Colloids Surf. B. Biointerfaces 85 (1) (2011) 2–7.
[46] K. Stellos, H. Langer, K. Daub, T. Schoenberger, A. Gauss, T. Geisler, B. Bigalke, I. Mueller, M. Schumm, I. Schaefer, P. Seizer, B.F. Kraemer, D. Siegel-Axel, A.E. May, S. Lindemann, M. Gawaz, Platelet-derived stromal cell-derived factor-1 regulates adhesion and promotes differentiation of human CD34+ cells to endothelial progenitor cells, Circulation 117 (2) (2008) 206–215.
[47] A. Peled, V. Grabovsky, L. Habler, J. Sandbank, F. Arenzana-Seisdedos, I. Petit, H. Ben-Hur, T. Lapidot, R. Alon, The chemokine SDF-1 stimulates integrin-mediated arrest of CD34(+) cells on vascular endothelium under shear flow, J. Clin. Invest 104 (9) (1999) 1199–1211.
[48] G. De Visscher, L. Mesure, B. Meuris, A. Ivanova, W. Flameng, Improved endothelialization and reduced thrombosis by coating a synthetic vascular graft with fibronectin and stem cell homing factor SDF-1alpha, Acta Biomater. 8 (3) (2012) 1330–1338.
[49] J. Yu, A. Wang, Z. Tang, J. Henry, B. Li-Ping Lee, Y. Zhu, F. Yuan, F. Huang, S. Li, The effect of stromal cell-derived factor-1α/heparin coating of biodegradable vascular grafts on the recruitment of both endothelial and smooth muscle progenitor cells for accelerated regeneration, Biomaterials 33 (32) (2012) 8062–8074.
[50] J.M. Anderson, A. Rodriguez, D.T. Chang, Foreign body reaction to biomaterials, Semin. Immunol. 20 (2) (2008) 86–100.
[51] T. Matozaki, Y. Murata, H. Okazawa, H. Ohnishi, Functions and molecular mechanisms of the CD47-SIRPalpha signalling pathway, Trends Cell Biol. 19 (2) (2009) 72–80.
[52] S.J. Stachelek, M.J. Finley, I.S. Alferiev, F. Wang, R.K. Tsai, E.C. Eckells, N. Tomczyk, J.M. Connolly, D.E. Discher, D.M. Eckmann, R.J. Levy, The effect of CD47 modified polymer surfaces on inflammatory cell attachment and activation, Biomaterials 32 (19) (2011) 4317–4326.
[53] J.B. Slee, I.S. Alferiev, C. Nagaswami, J.W. Weisel, R.J. Levy, I. Fishbein, S.J. Stachelek, Enhanced biocompatibility of CD47-functionalized vascular stents, Biomaterials (2016) 8782–8792.

Supplementary Information for

Linker-free Covalent Immobilization of Heparin, SDF-1α, and CD47 on PTFE Surface for Antithrombogenicity, Endothelialization and Anti-inflammation

Ang Gao[a,b], Ruiqiang Hang[c], Wan Li[a], Wei Zhang[d], Penghui Li[b], Guomin Wang[a], Long Bai[c], Xue-Feng Yu[b], Huaiyu Wang,[b,*] Liping Tong,[b,*] and Paul K Chu[a,**]

[a] *Department of Physics and Materials Science, City University of Hong Kong, Tat Chee Avenue, Kowloon, Hong Kong, China*
[b] *Institute of Biomedicine and Biotechnology, Shenzhen Institutes of Advanced Technology, Chinese Academy of Sciences, Shenzhen 518055, China*
[c] *Research Institute of Surface Engineering, Taiyuan University of Technology, Taiyuan 030024, China*
[d] *Technical Institute of Physics and Chemistry, Chinese Academy of Sciences, Beijing 100190, China*

* Corresponding authors at: Institute of Biomedicine and Biotechnology, Shenzhen Institutes of Advanced Technology, Chinese Academy of Sciences, Shenzhen 518055, China.
** Corresponding author at: Department of Physics and Materials Science, City University of Hong Kong, Tat Chee Avenue, Kowloon, Hong Kong, China.
Email addresses: paul.chu@cityu.edu.hk (P.K. Chu), hy.wang1@siat.ac.cn (H. Wang), lp.tong@siat.ac.cn (L. Tong)

Materials and Methods

1. HRP immobilization and quantification

HRP possessing activity that could be easily monitored by reacting with the chromogenic substrate such as 3,3',5,5'-tetramethylbenzidine (TMB) was employed as a model protein to confirm that proteins could be covalently immobilized on the N2 samples by simple incubation in solutions. Since the N2 samples were apparently superhydrophobic, they were degassed in an ultrasonic bath in PBS solution prior to the incubation with HRP. The PTFE and N2 samples (as prepared and stored under ambient conditions for 72 and 198 days) were immersed in a 50 μg/ml HRP solution for 12 hours at 4 °C. Afterwards, the samples were taken out, rinsed with PBS, eluted with 2% SDS solution for 1 hour, and then added with 0.5 ml of the TMB solution for color development. After 3 minutes, the chromogenic reaction was stopped by addition of 0.5 ml of 2 M HCl. The mixture of each sample was collected and the absorbance at 450 nm was determined spectrophotometrically.

2. Determination of SDF-1α

The released and immobilized SDF-1α from N2-Hep-SDF and N2-Hep-SDF-CD47 samples after incubation with PBS solution for 1, 3, and 5 days was determined using a commercial ELISA kit according to the manufacturer's protocols. Briefly, to quantify the amount of released SDF-1α, a monoclonal antibody specific to SDF-1α was pre-coated on the bottom of a 96-well plate and then the solutions containing released SDF-1α were pipetted into the wells and incubated at 37 °C for 2 hours.

Afterwards, each well was rinsed, incubated with the enzyme-linked polyclonal antibody specific to SDF-1α, and reacted with a substrate solution, and the absorbance was monitored on a microplate spectrophotometer (Eon, Biotek, USA). The amount of released SDF-1α was calculated according to the standard curve prepared with the standard SDF-1α solutions. To quantify the amount of immobilized SDF-1α, the N2-Hep-SDF and N2-Hep-SDF-CD47 samples were directly incubated with the enzyme-linked polyclonal antibody specific to SDF-1α and reacted with a substrate solution. The absorbance was determined spectrophotometrically and the amount is calculated according to the standard curve.

3. EPC phenotype

The phenotype of cells was examined by immunofluorescence staining of the surface markers including CD34, CD133, Flk-1, and CXCR4. Briefly, the cells after incubation for 7 days were fixed with 4% PFA for 10 minutes and permeabilized with 0.5% Triton X-100 for 20 minutes prior to the immunofluorescence staining. After being blocked with 1% BSA for 30 minutes, the cells were incubated with the primary rabbit anti-CXCR4 antibody, mouse anti-Flk-1 antibody, rabbit anti-CD34 antibody, and rabbit anti-CD133 antibody at 4 °C overnight, respectively. Subsequently, the cells were rinsed with PBS, and incubated with the corresponding secondary antibodies (FITC conjugated anti-mouse IgG, FITC conjugated anti-rabbit IgG, or CY3 conjugated anti-rabbit IgG) for 60 minutes at room temperature. In addition, the cell

nuclei were stained with hoechst for 5 minutes and examined by fluorescent microscopy (Axio Observer Z1, Carl Zeiss, Germany).

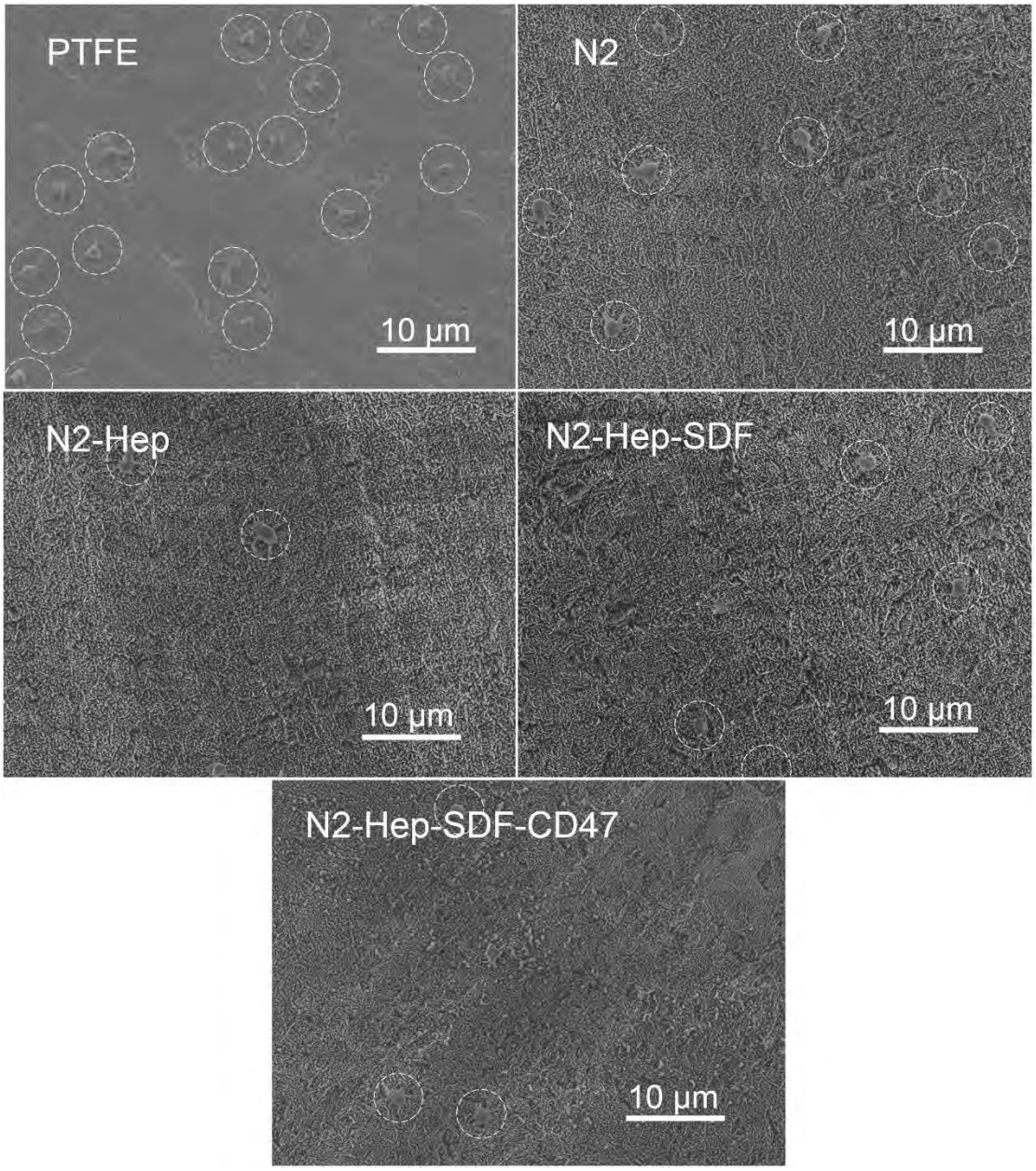

Fig. S1 Representative SEM images of adherent platelets on each sample after incubation for 1 hour with PRP.

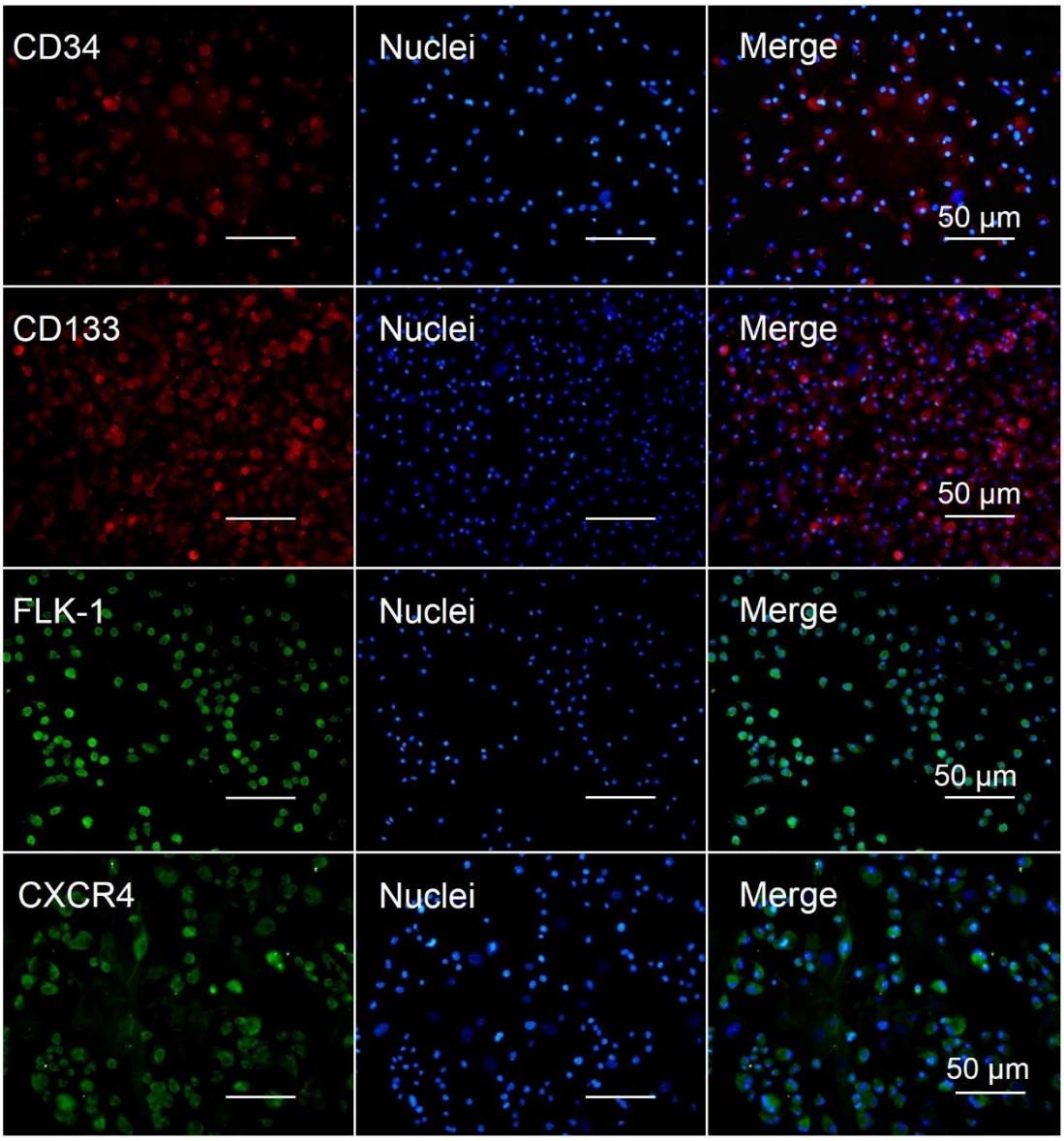

Fig. S2 Phenotype characterization of isolated EPCs by immunofluorescence staining CD34, CD133, Flk-1, and CXCR4.

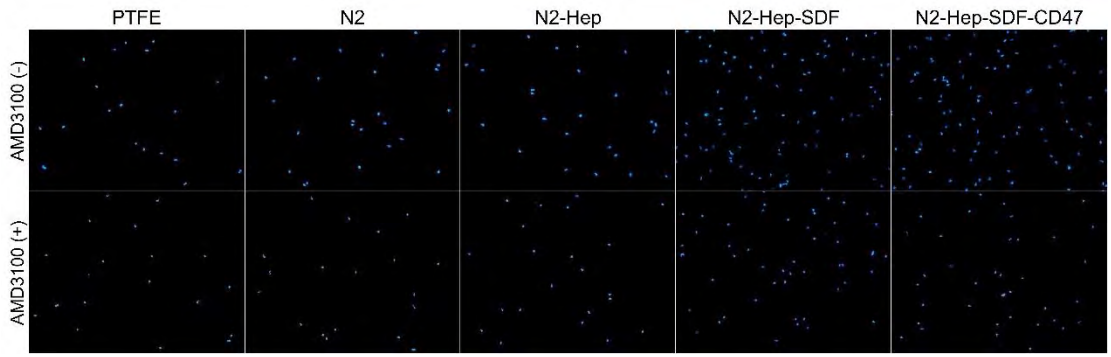

Fig. S3 Representative DAPI-stained fluorescent images of EPCs adhering on each sample before and after the treatment with AMD3100.

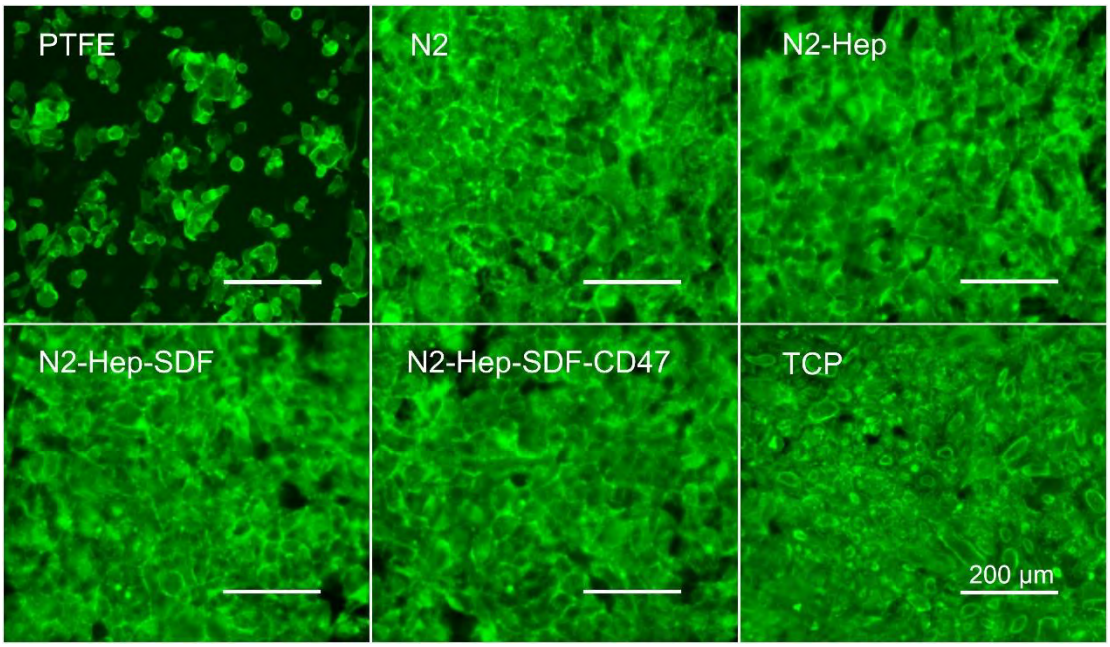

Fig. S4 Representative fluorescent images of the HUVECs on each sample and TCP positive control after incubation for 3 days. Note that the cells on PTFE cannot reach confluence.

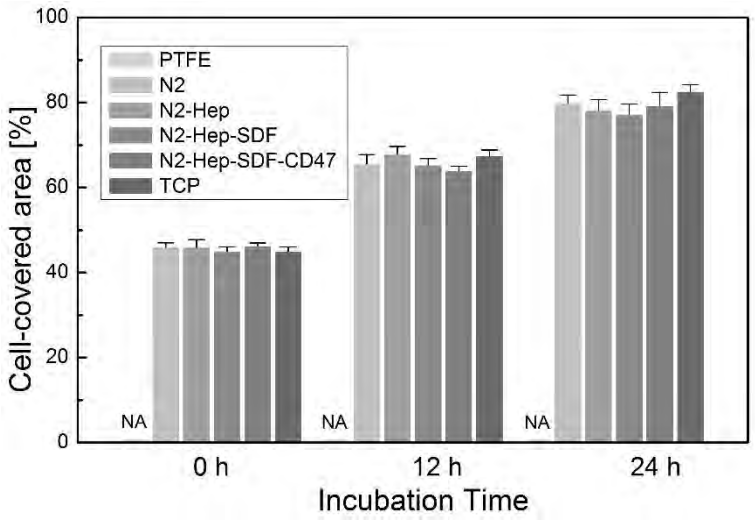

Fig. S5 Quantification of HUVECs migration on each sample and TCP positive control into the cell-free gap zone (500 μm in width) after incubation for 0, 12, and 24 hours. The corresponding results of the PTFE group are void.

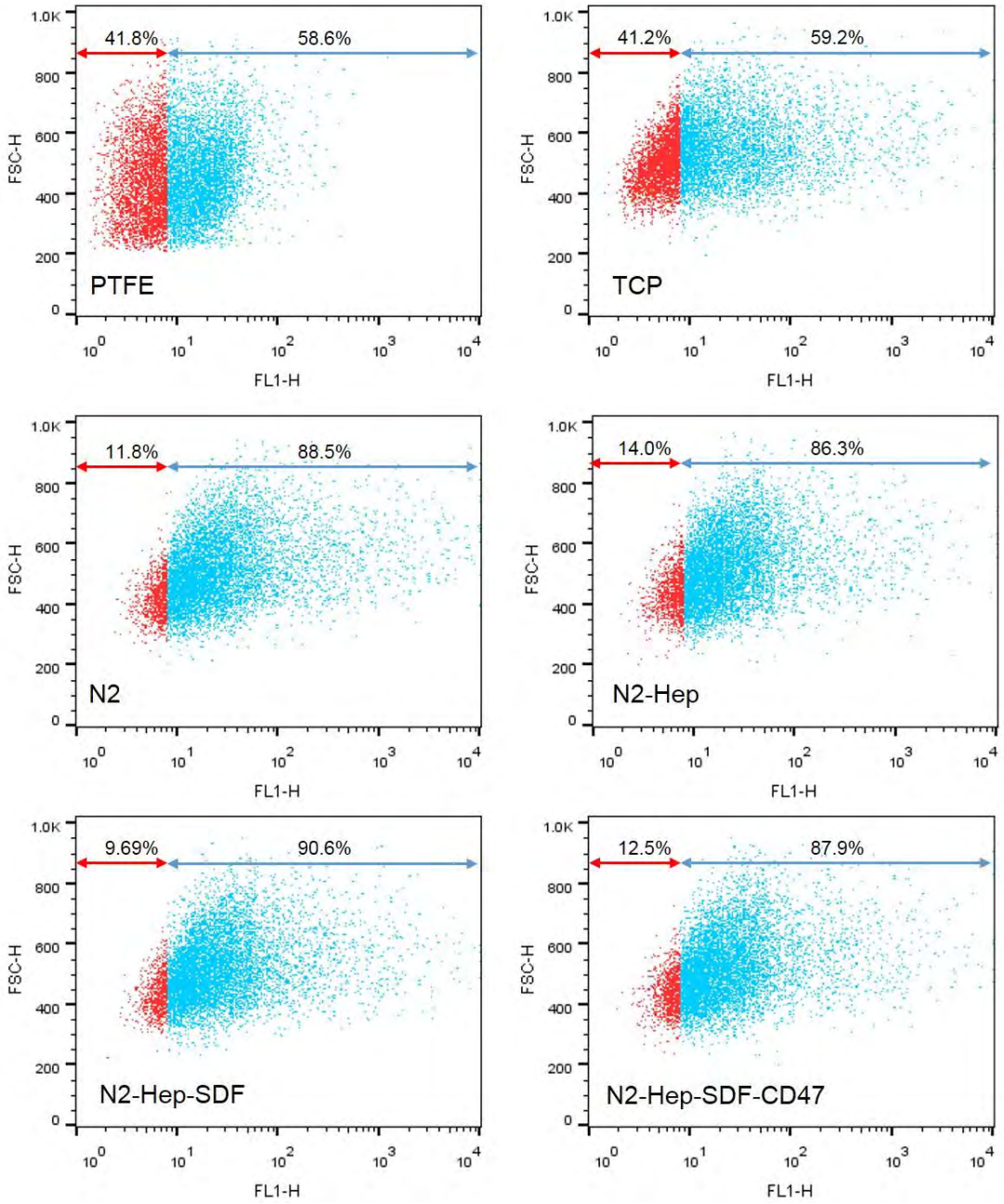

Fig. S6 Flow cytometry analysis of NO secretion of HUVECs on each sample and TCP positive control after incubation for 48 hours. The blue dots are referred to NO-positive cells and red dots to NO-negative cells.

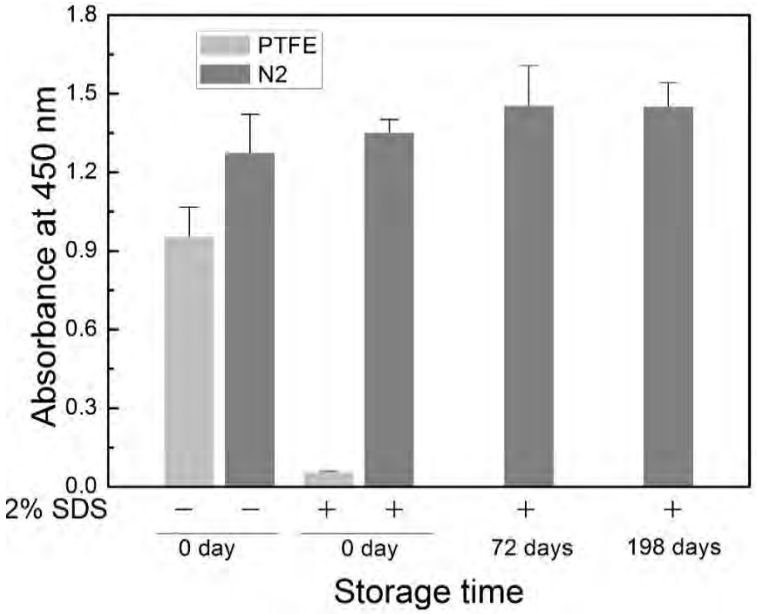

Fig. S7 Relative amounts of HRP loaded on the pristine PTFE and N2 samples after storage under ambient conditions for 0, 72, and 198 days. (- referred to the results before 2% SDS elution and + referred to the results after 2% SDS elution).